

BELLCOMM, INC.

SUBJECT: A Critical Look at the Martian
Atmosphere - Case 103-2

DATE: October 26, 1966

FROM: M. Liwshitz

ABSTRACT

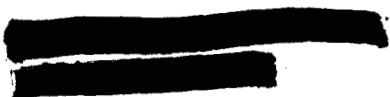
A broad survey of present knowledge of the Martian atmosphere is presented. The gradual accumulation of information obtained before the Mariner IV flyby is reviewed, and the methods of investigation are briefly discussed. The Mariner IV results, and conclusions drawn from these, are considered in detail. Throughout this survey an attempt is made to distinguish between results of direct observation and conclusions based on theories yet in need of empirical confirmation of their underlying assumptions.

(NASA-CR-153689) A CRITICAL LOOK AT THE
MARTIAN ATMOSPHERE (Bellcomm, Inc.) 30 p

N79-73376

Unclas
00/91 12389

FACILITY FORM 002	X 67-35498	X 67-70959
	(ACCESSION NUMBER)	(THRU)
	31	2A
	(PAGES)	(CODE)
	CR-80985	30
	(NASA CR OR TMX OR AD NUMBER)	(CATEGORY)



SUBJECT: A Critical Look at the Martian
Atmosphere - Case 103-2

DATE: October 26, 1966

FROM: M. Liwshitz


MEMORANDUM FOR FILE

I. INTRODUCTION

Atmospheric structure of a planet is roughly defined by the altitude profile of very few thermodynamic parameters. These are temperature, pressure, mass and number density. To take account of chemical composition, both partial and total pressures have to be considered. Through interaction with the solar energy flux, and by their mutual interplay, a profile of these parameters evolves which serves as an adequate model of an average static atmosphere for most engineering purposes. In some instances (e.g., the effect of winds on landing operations) certain dynamic processes have to be considered; analysis of others, such as, for example, ionospheric phenomena, may also be required for a clearer insight into the structure of even the static atmosphere.

Prior to exploration with in situ probes carried aloft by high altitude rockets and satellites, knowledge of the earth's atmosphere was sparse and subject to large uncertainties in some areas, such as, e.g., the temperature profile and composition at altitudes above 100 km. In the absence of direct close-by observation, knowledge of planetary atmospheres was based exclusively on results of astronomical investigations, limited to the narrow windows of the electromagnetic spectrum accessible through the terrestrial atmosphere.

For Mars these observations provided a fairly reliable estimate of surface temperature, determining the latter within about 20% of 240°K. This value of surface temperature, averaged over the sunlit disk, and widely accepted before Mariner IV⁽¹⁾ (2), is, indeed, in good agreement with the determination of near surface temperature deduced from the results of this recent experiment. It is probably very close to the value that an in situ thermometer will determine in the future. Moreover, scans over the sunlit disk provided insight into the diurnal temperature variation which appears to display an amplitude of ~50°K on either side of the central value indicated.



On the other hand, Mariner IV results revealed that previous estimates of composition and pressure were far off the mark. Astronomical observations had led to qualitative identification of some chemical components of the Martian atmosphere, such as carbon dioxide and water vapor. For CO_2 a lower abundance limit of $\sim 10 \text{ gm cm}^{-2}$ had been obtained from careful analysis of Martian spectra^{(4) (5)}. The presence of water vapor in the Martian atmosphere had also been clearly established; but its quantity was (and still is) subject to large uncertainty, estimates ranging from $\sim 1.4 \times 10^{-3} \text{ gm cm}^{-2}$ ⁽⁴⁾ to $2 \times 10^{-2} \text{ gm cm}^{-2}$ ⁽⁶⁾. For other components, such as CO and O_2 , only upper abundance limits could be ascertained*. But for years the accepted model of the Martian atmosphere assumed, in analogy with the earth, a preponderance of nitrogen in this planet's atmospheric composition, though, owing to its spectroscopic inertness, nitrogen could never be directly identified. The accepted value of surface pressure centered around $\sim 85 \text{ mb}$.

The Mariner IV occultation experiment confirmed the earlier estimate of CO_2 abundance, but indicated that CO_2 is the major constituent of the Martian atmosphere. It also revised drastically the estimate of surface pressure, which is now thought to be about 5-10 mb, an order of magnitude below the value indicated above.

In view of the paucity of unambiguous empirical data, great latitude existed for the construction of atmospheric models for Mars^{(7) (8) (9) (10)} aiming at a description of its temperature and density profile. In general these models, starting from questionable assumptions, led to wrong conclusions.

The Mariner IV occultation experiment yielded the first glimpse into the actual structure of the Martian atmosphere by obtaining data which refer to different distinct regions of the atmosphere. This is in contrast to all previous astronomical studies which, apart from those of surface and subsurface temperature, inevitably observed effects integrated over the whole of the planet's gaseous envelope, and therefore were amenable to great ambiguities in interpretation.

The fundamental character of the Mariner IV results and the relatively high accuracy of the deduced structural parameters is evident from Table 1, adapted from Fjeldbo, G., et al⁽¹¹⁾.

*Recent reports on results of spectroscopic observations of Mars with a high resolution interferometer (Connes, J., P. Connes, and L. D. Kaplan, Science, 153, 739, August 1966) indicate the presence of a surprisingly high fraction ($\sim 10^{-3}$) of methane derivatives in the Martian atmosphere.

TABLE I

SUMMARY OF STRUCTURAL PARAMETERS OBTAINED FROM THE
MARINER IV OCCULTATION EXPERIMENT AT IMMERSION

Surface Number Density	$2.05 \pm 0.25 \times 10^{17} \text{ cm}^{-3}$
Surface Mass Density	$1.50 \pm 0.15 \times 10^{-5} \text{ gm cm}^{-3}$
Surface Scale Height	$9.0 \pm 1.0 \times 10^5 \text{ cm}$
Surface Pressure	$5.1 \pm 1.1 \text{ mb}$
Near Surface Temperature	$175 \pm 25^\circ \text{K}$
Electron Density at $120 \pm 5 \text{ km}$	$9.5 \pm 1.0 \times 10^4 \text{ cm}^{-3}$
Electron Density at $\sim 100 \text{ km}$	$\sim 2.5 \times 10^4 \text{ cm}^{-3}$
Plasma Scale Height above	
Electron Peak	$2.4 \pm 0.3 \times 10^6 \text{ cm}$

These results put man's knowledge of the Martian atmosphere on a much firmer basis than available hitherto, and have reduced to a considerable degree the permissible latitude in bridging between the known values of structural parameters and extrapolating from them. Still there exists a wide range of possible interpretation^{(11) (12) (13) (14) (15)}.

It can be stated with confidence, however, that upon completion of advanced Martian missions employing direct atmospheric probes, which are now under consideration, knowledge of the Martian atmosphere will advance to a stage not dissimilar to that pertaining to the terrestrial atmosphere today.

II. A SURVEY OF PRE-MARINER IV ATMOSPHERIC DATA ON MARS

As indicated in the introduction, a planet's surface temperature is the atmospheric parameter most easily accessible to direct measurement. This statement is, however, in need of some qualification in the presence of a sizeable atmosphere interacting strongly with solar radiation. The surface whose

temperature is purportedly measured becomes ill defined and is not necessarily the planet's actual surface, but may be an atmospheric layer of altitude varying with wavelength. Moreover, the thick atmospheric layer brings about a blanketing effect which may profoundly alter the thermal balance near the surface. This is well exemplified by the Cytherean atmosphere, where heavy cloud layers obstruct direct transmission of solar radiation over broad regions of the spectrum.

Fortunately, from this point of view, Mars does not possess a heavy atmosphere, and it has been possible, therefore, to determine Martian surface temperatures from earth based observations with satisfactory accuracy.

In this case even the simplest method based on the Stefan-Boltzmann law yields a fairly reliable estimate. On the average, the solar radiation energy absorbed by the sunlit disk (of area πr^2), the bulk of which is in the visible and near infrared portions of the spectrum, equals the thermal radiation emitted by the planet's total surface (of area $4\pi r^2$),

$$\text{i.e.} \quad f(1-a) = 4\sigma T^4 \quad (1)$$

or

$$T = [f(1-a)/4\sigma]^{1/4} \quad (2)$$

Here $f \approx 6.0 \times 10^5 \text{ erg cm}^{-2} \text{ sec}^{-1}$ is the solar energy flux at the mean heliocentric distance of Mars, $\sigma \approx 5.7 \times 10^{-5} \text{ erg cm}^{-2} \text{ sec}^{-1} \text{ }^\circ\text{K}^{-4}$ is the Stefan-Boltzmann constant, $a \approx 0.15$ is the mean visual albedo of Mars. Inserting these values into Equation (2) yields

$$T \approx 220^\circ\text{K}$$

As will be seen below this value is too low by about 10%. The main sources of error in this simple estimate stem from the application of the Stefan-Boltzmann law, assuming the Martian surface to behave as a black body radiator (in the infrared), and from the averaging of the Martian albedo, which displays strong variations with wavelength.

Whereas in the method just described, the surface temperature is inferred from optical measurement of the albedo via some assumptions about the radiative properties of Mars, it can be measured directly using various methods of radiometry which are based on Planck's law. An extended series of observations by Sinton and Strong⁽¹¹⁾ ⁽¹⁶⁾ in the infrared yielded quite detailed temperature curves with relatively high spatial resolution of the surface ($\sim 1/15$ of the planet's disk). The only significant error in the reduction of results in this type of measurement lies in the assumption of unit emissivity for the Martian surface, which may cause an underestimate of the actual temperatures by no more than 5%.*

Direct results of the above observations revealed a variation of surface temperature at the Martian equator from $\sim 210^\circ\text{K}$ at 0700 a.m. Martian local time to $\sim 295^\circ\text{K}$ at noon. Extrapolation by means of the equation of heat conduction yielded a minimum temperature near $\sim 200^\circ\text{K}$, and a corresponding maximum of $\sim 300^\circ\text{K}$. This would yield a rough average temperature of $\sim 250^\circ\text{K}$.

Sinton and Strong's observations appear to be a reliable measurement of surface temperature, really no worse than most terrestrial measurements. Three points are noteworthy with respect to these results:

- (a) The daytime surface temperatures of dark areas appear to be about $\sim 8^\circ\text{K}$ higher than those of lighter areas.
- (b) The large amplitude of temperature variations indicates very low thermal inertia, $(k\rho c)^{1/2}$ (where k is the thermal conductivity, c the specific heat, and ρ the mass density of the surface). This in turn suggests a loose, dry, grainy structure of surface soil⁽¹⁷⁾.
- (c) In analogy with dry, sandy regions of the earth it is believed⁽¹⁸⁾ that the near surface temperature

* Strictly speaking, the possession of a finite albedo precludes consideration of a planet as a black body. Since, however, the bulk of solar radiation which is absorbed (and reflected) is in a region of the spectrum that does not overlap the spectral range over which the thermal radiation is emitted, one might still consider the planet as a black body emitter of long wave radiation. If this assumption is dropped and an emissivity $\epsilon < 1$ is adopted, the observed radiation intensity becomes $\epsilon \sigma T^4$, such that for $\epsilon \approx 0.8$, $T \approx \epsilon^{-1/4} T_b \approx 1.05 T_b$ with T_b the black body temperature corresponding to the same radiation intensity.

of Mars is $\sim 50^\circ$ lower than the values quoted. This is based on the empirical relation that the minimum near surface temperature is close to the surface minimum, while the amplitude of its variation is only a fraction, $< 1/2$, of the surface temperature variation. Consequently the atmospheric temperature near the ground is $\sim 200^\circ\text{K}$. Table I shows this estimate to be well borne out by the Mariner IV results.

Radiometric observations have also been carried out in the cm wave region⁽¹⁹⁾, yielding $\sim 210 \pm 20^\circ\text{K}$ for the temperature of the subsurface, which has to be considered the main emitting region in this wavelength region. The above subsurface radio temperatures appear to be consistent with the measured surface temperatures.

Measurements of the temperature near the surface and the identification of some chemical components, mentioned in the introduction, exhaust the store of firm empirical knowledge about the Martian atmosphere available prior to the Mariner IV flyby. Other statements on its structure leaned heavily on theoretical considerations. In the absence of empirical data to test their underlying assumptions, theoretical calculations appear to have led in many instances to erroneous quantitative estimates on the structural parameters. Evidently the degree of error was in direct proportion to the range of phenomena these theories sought to describe.

This is demonstrated by the results of a calculation on the location of the Martian tropopause, which in a reasonably simple manner led to a value of the former's altitude in fair agreement with that deduced from Mariner IV results. Under the assumptions of this theory^{(21) (22)}, the atmosphere consists of a lower layer in convective (adiabatic) equilibrium, the troposphere, and an upper isothermal layer, the stratosphere, in radiative equilibrium with constant temperature T_s . In the troposphere the lapse rate of temperature is the constant adiabatic lapse rate α_t , where

$$\frac{dT}{dz} = - \frac{g}{C_p} = \alpha_t$$

$g(\text{cm sec}^{-2})$ is the gravitational acceleration near the surface of the planet; $C_p(\text{erg}^\circ\text{K}^{-1})$ is the specific heat of the atmospheric gas. For Mars $g \approx 3.75 \times 10^2 \text{ cm sec}^{-2}$, and for most gases of interest (N_2 , CO_2), $C_p \approx 10^7 \text{ erg } ^\circ\text{K}^{-1}$, so that

$$\alpha_t = -3.75^\circ\text{K/km} \quad (3)$$

Let h be the altitude of the tropopause; then T_s , the stratospheric temperature, is given by

$$T_s = T_o - \alpha_t h \quad (4)$$

with T_o the temperature at the base of the troposphere (near ground). Neglecting direct absorption of solar radiation by a volume element of unit area in the stratosphere, its radiation balance is expressed by the following equation:

$$2\sigma T_s^4 = \sigma T_o^4 \quad (5)$$

Both surfaces of the volume element emit radiation at T_s , while only its lower surface absorbs radiation at T_o . Combining equations (4) and (5) one obtains

$$h = (1 - 2^{-1/4}) T_o / \alpha_t \quad (6)$$

With $T_o \approx 200^\circ\text{K}$, this gives $h \approx 8.5$ km and $T_s \approx 168^\circ\text{K}$. While this value of h appears quite reasonable, it cannot be determined from present data. The temperature of $\sim 170^\circ\text{K}$ in the lower stratosphere appears to be in the right order (within $\sim 15\%$), as is borne out by more sophisticated calculations based on the simultaneous numerical solution of the equation of radiative transfer and the equation of hydrostatic equilibrium^{(7) (9) (10)}. Though solution of these equations requires certain assumptions about the chemical composition of the atmosphere (as this determines the interaction with solar radiation), the results on the temperature structure in the lower atmosphere are not overly sensitive to the initial assumptions. This is not the case, however, with respect to higher altitudes (above ~ 50 km), where radiative equilibrium is inhibited by the low collision frequency, and where composition plays a decisive role. This is evident from the results of radiative transfer calculations on Martian model atmospheres quoted, yielding limiting temperatures for the critical level, the base⁽⁹⁾ of the collisionless exosphere, varying between 500° and 3500°K . Even after Mariner IV this is still a highly controversial subject^{(5) (11) (13) (14) (15)}.

Another area of great uncertainty up to the Mariner IV flyby was the problem of pressure. Though observational astronomy provides a number of methods for probing the pressure of planetary atmospheres, interpretation of observational results depends heavily on assumptions about the atmosphere and has, therefore, led to widely diverging results.

The simplest methods are polarization studies and photometry. In the former the polarization of light reflected from the planet is measured at different zenith angles (see Figure 1). This enables separation of the respective contributions of the atmosphere and the surface. The contribution to light intensity from the atmosphere can then be converted into pressure. The sources of uncertainty in this method are assumptions about the scattering process in the atmosphere, and the composition, which determines the polarizability of the medium. A significant proportion of aerosols or microscopic particles in the atmosphere would contribute non-Raleigh scattering. The effect of the uncertain assumptions can be sensed from the wide range of surface pressures which may be deduced from polarization measurements, 30-200 mb⁽⁵⁾. Similar problems are encountered in photometric determinations of pressure, where the respective contributions of surface and atmosphere to the light intensity are separated by studying the spatial and diurnal variation in brightness. Again the relative contribution of particles of different size has to be determined before the empirical data can be interpreted. The range of pressures derived from this method varies, therefore, between 60-110 mb.

The most accurate method of pressure determination is the spectroscopic method, to be discussed now in more detail^{(23) (24)}. As the spectrum of light from a planet is scanned, absorption lines appear, and it is possible to measure the so-called equivalent width of these lines - which is the width (in angstrom or frequency units) of a completely black line that would subtract from the continuum the same amount of energy as does the real line. To permit evaluation of the dependence of this empirical quantity on the relevant parameters the equivalent width of a line is defined as

$$W = \int_{\Delta\nu} (1 - e^{-K_\nu u}) d\nu \quad (7)$$

K_ν is the appropriate absorption coefficient at a frequency ν ; it is expressed in units according to the measure of the amount of absorbing material u in the optical path. E.g. if u is expressed in gm cm^{-2} , the dimensions of K_ν are $\text{gm}^{-1} \text{cm}^2$. Whatever the dimensions of u , evidently

$$u \propto N,$$

the number of absorbing molecules in the path of observation.

One may express K_ν as a product

$$K_\nu = S f(\nu) \quad (8)$$

where S is the so-called line intensity, and $f(\nu)$ the form factor, which is normalized such that

$$\int_{-\infty}^{\infty} f(\nu) d\nu = 1 \quad (9)$$

Also $S \propto f$, where f is the effective number of electrons per molecule with natural frequency ν , the so-called oscillator strength.

Of wide use in astronomical applications is the assumption that $f(\nu)$ is the Lorentz shape factor

$$f(\nu) = \frac{\alpha/\pi}{(\nu - \nu_0)^2 + \alpha^2} \quad (10)$$

with ν_0 the center of the line and α the damping factor, which depends on the characteristic time of damping of the incident wave. If this is effected by collisions, then

$$\alpha \propto (P/T)^{1/2} \quad (11)$$

Given $f(\nu)$ one may evaluate the integral Equation (7). For $f(\nu)$ as in Equation (10) this can be done quite conveniently in the limit $Su/\alpha \rightarrow 0$ (the weak line approximation). One obtains upon substitution $x = (\nu - \nu_0)/\alpha$, and $\xi = Su/\alpha$

$$W = \alpha \int_{\Delta x} (1 - e^{\xi f(x)}) dx \approx \alpha \xi \int_{-\infty}^{\infty} f(x) dx = \alpha \xi$$

$$\text{or} \quad (12)$$

$$W \propto Su = AN$$

For the so-called strong line or square root approximation, for $Su/\alpha \rightarrow \infty$, a somewhat more complicated integration can be shown⁽²³⁾ to lead to

$$W \propto (Su)^{1/2} = B(NP)^{1/2} \quad (13)$$

where A is a constant and B depends on T. Thus, by measuring the line width of both a weak and a strong line one may, in principle, determine both the total abundance of the absorbing gas in a planetary atmosphere, and its total surface pressure assuming some atmospheric profile. Unfortunately, hidden sources of error limit the validity of results derived from this method: 1) overlap of a number of lines, 2) overlap with solar Fraunhofer lines, 3) overlap of Martian and terrestrial absorption lines, 4) uncertainties in the temperature of the absorbing gas, 5) uncertainties in the line shape, determining the relation between pressure and line broadening, 6) uncertainty in composition, which affects line broadening by collision of particles of different species. Some check on these errors can be obtained from experimental curves of growth, yielding the dependence of line width on the depth of absorber, but what appears to be amenable to relatively precise determination are limiting pressures and abundances.

When this method was applied to the Martian atmosphere by utilizing the weak absorption bands of CO_2 at 8700 Å, together with the strong, pressure dependent bands at 1.57 and 1.6 μ , the resulting minimum pressures varied between 4.2⁽²⁵⁾ and 6.4 mb⁽⁴⁾ ⁽²⁵⁾, on the assumption that the Martian atmosphere is pure CO_2 . Though these values are close to those deduced from the Mariner IV flyby, they were not seriously considered prior to this mission, but only regarded as quite remotely possible lower limits.

In summarizing the state of knowledge before mid-1966 it can be stated that the only atmospheric parameter known with a high degree of confidence, say 20%, was the surface temperature. The lowest portion of the temperature profile was probably estimated correctly. Estimates of surface pressure varied by almost 2 orders of magnitude (from ~ 4 to ~ 200 mb), and no reliable statement could be made on the profile of temperature, density, pressure and composition.

III. THE MARINER IV RESULTS AND THEIR INTERPRETATION

A significant advance in the state of knowledge about the Martian atmosphere came with the publication of the results of the Mariner IV occultation experiment⁽³⁾. Though an active controversy still persists on the interpretation of the data with respect to the structure of the upper atmosphere, a number of important questions appears now to be settled, such as the order of magnitude of the surface pressure and the peak electron density in the ionosphere, the surface temperature, and the basic chemical composition of the atmosphere. Consequently the range of assumptions for theoretical studies has been considerably narrowed down, and aims for further experimental probing of the atmosphere can now be much better defined.

The physical basis of the occultation experiment is the refraction of radiation by the atmosphere and ionosphere^{(26) (27) (28)}: 1) the radio propagation velocity ceases to be the free space velocity c ; 2) the radial gradient in atmospheric density, and hence in the refractivity, bends the path and produces an apparent change in signal transmitter velocity; 3) the refractive defocusing causes a change in signal strength received at earth. There are additional effects, but these will not be discussed here since they were not utilized in the occultation experiment. The above effects produce conveniently measurable quantities: 1) and 2) change the effective path length for transmission from the flyby vehicle and cause a residual delay in reception of the signal at the earth, compared to that expected in absence of an atmosphere. This time delay may be expressed in terms of a phase shift $\Delta\phi$ cycles. The change in signal velocity produces a residual Doppler shift, Δf cycles/sec, compared to that caused⁽³⁾ by the vehicle's motion in free space. The change in attenuation can be measured directly in terms of ΔA db.

Upon certain plausible assumptions, such as an exponential, spherically symmetric atmosphere, these measured quantities are simply related to atmospheric parameters. For signal propagation paths just grazing the surface of the planet one obtains⁽²⁷⁾

$$\Delta\phi = \frac{1}{\lambda} (\mu_s - 1) (2\pi R_p)^{1/2} H^{1/2} \quad \text{cycles} \quad (14)$$

$$\Delta f = \frac{1}{\lambda} (\mu_s - 1) (2\pi R_p)^{1/2} H^{-1/2} v_s \quad \text{cycles/sec} \quad (15)$$

$$\Delta A = -4.34(\mu_s - 1) \mu_s (2\pi R_p)^{1/2} H^{-3/2} \quad \text{db} \quad (16)$$

Here λ is the radar wavelength employed, μ_s is the index of atmospheric refraction at the surface, R_p cm is the planet's radius, H cm the atmospheric scale height, and v_s cm/sec the spacecraft's velocity at flyby. μ_s is simply related to the atmospheric surface density, and depends on composition. Analogous relations can be obtained for the dependence of $\Delta\phi$, Δf , ΔA on ionospheric parameters⁽²⁹⁾.

The maximum values of $\Delta\phi$, Δf , and ΔA reported from the Mariner IV experiment were

$$\Delta\phi_m = 29 \pm 2 \text{ cy}$$

$$\Delta f_m = 5.5 \pm 0.5 \text{ cy/sec}$$

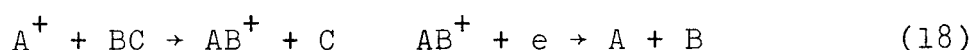
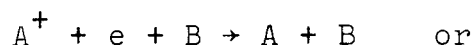
$$\Delta A_m = 1.5 - 2.0 \text{ db}$$

Figure 2 from⁽³⁾ relates these values to surface refractivity, $N_s = (\mu_s - 1) \times 10^6$, and scale height of an exponential atmosphere and indicates the possible range of these values. Figure 3, also from⁽³⁾, shows the dependence of refractivity on density and composition. From these results and analogous data on the ionosphere Table I in the introduction was compiled. Figure 4 presents these results in graphical form as a function of altitude.

It should be noted that the values in Table I were derived from the data at immersion. Diffraction effects indicate that this took place over an elevated feature of Mars, suggesting that pressure and density may not refer to Martian "sea level". Elevation introduces a change of 1%/90m in these parameters and the uncertainty is reflected in Figure 4.

To obtain a complete model of the Martian atmosphere one has now to bridge over the large gaps between the "known" portions of Figure 4, which include: 1) pressure, density and temperature at the surface and near it, 2) an exponential electron density profile above a peak near ~ 120 km with a scale height of ~ 25 km, 3) a steeper density gradient below this peak and possibly a secondary peak at ~ 100 km, and 4) nighttime electron density $< 10^3 \text{ el. cm}^{-3}$. To do so, one has again to leave the firm ground of empirical data and enter the realm of plausible conjecture. Since at high altitudes (~ 100 km) the density and temperature profiles of the neutral atmosphere are not known, one attempts to relate them to the known electron profile by considering ionospheric processes, in analogy with phenomena in the terrestrial atmosphere.

The ionosphere is formed by the interplay of photo-ionization of atmospheric molecules and their recombination with the free electrons formed, mainly in three body collision processes. Schematically these processes are described by



Here A, B, C denote gas molecules, e denotes an electron, and $h\nu$ a photon. Direct recombination, $A^+ + e \rightarrow A$, is not effective because of the stringent conditions on the energy of the neutral molecules, which is restricted to discrete states. On top of these collision processes diffusion may affect the structure of the ionosphere.

The two principal stable layers in the terrestrial ionosphere are the E and F regions. The former extends from ~ 85 to ~ 150 km altitude, in the range where N_2 , O_2 , and O are the major atmospheric constituents; the principal ionizing agents are thought to be soft solar X-rays ($\sim 10 - 200$ Å) and some UV in the regions between $\sim 800 - 1027$ Å. The E region displays strong diurnal variation, its electron density at ~ 150 km varying from $\sim 10^5 \text{ cm}^{-3}$ to $\sim 10^3 \text{ cm}^{-3}$ from day to night. It can be shown on the basis of simple layer theory⁽²⁹⁾, which may be applied to the E layer, that its peak occurs at unit optical depth, i.e., where

$$\sigma n H \sec x = 1 \quad (19)$$

Here $n \text{ cm}^{-3}$ denotes the number density of neutral molecules, H cm their scale height, x radians the zenith angle of solar radiation, and $\sigma \text{ cm}^2$ is the photoionization cross section.

This simple theory cannot be applied to the more complex F layer, where plasma diffusion plays an important role. In the terrestrial atmosphere the F layer displays two distinct peaks in electron density in the daytime. The lower F_1 peak near ~ 180 km occurs in the region of maximum electron production, with a characteristic electron density of $\sim 3 \times 10^5 \text{ cm}^{-3}$ at noon and

$\sim 10^4 \text{ cm}^{-3}$ after sunset. The higher F_2 peak near $\sim 350 \text{ km}$ evolves as a result of the low density of neutral particles at high altitudes which inhibits recombination. The diurnal variation from $\sim 10^6$ to 2.5×10^5 is less pronounced than that of either the F_1 and E layer. The reduced variation is a consequence of slow recombination and diffusion. Above the F_2 peak diffusion processes become dominant and therefore this maximum will roughly be located where the time scale for diffusion and loss by recombination become equal, i.e.

$$\beta = D/H^2 \quad (20)$$

Here $\beta \text{ sec}^{-1}$ is the loss coefficient for ions in the F_2 region; $H^2/D \text{ sec}^{-1}$ is the diffusion time, with $D \text{ cm}^2 \text{ sec}^{-1}$ the diffusion coefficient. Above its peak the density profile of the F_2 layer is roughly exponential, typical of diffusive equilibrium.²

It is evident that the formation of the ionosphere is strongly affected by the chemical composition of the neutral atmosphere, since ionization thresholds and cross sections vary from species to species, and the effective recombination of ions depends on the ambient neutral density.

From the brief description of the terrestrial ionosphere it appears quite natural that some of the investigators assumed the observed peak in the Martian atmosphere to be an F_2 type peak^{(11) (13)}. As it impinges on the atmosphere, the solar UV flux will be attenuated by ionizing and dissociating the ambient neutral molecules and atoms. The big question at this point is which species of neutral particles will be predominant at small optical depths. Since CO_2 is likely to be the major constituent of the Martian atmosphere, with possible admixture of N_2 and A, and the dissociation threshold of CO_2 is $\sim 1690 \text{ \AA}$, the following constituents may occur at high altitudes: N_2 , A, CO_2 , CO, O_2 , O. In view of its smaller molecular weight there must be a level above which atomic oxygen predominates because of diffusive separation, like in the terrestrial atmosphere above the turbopause at $\sim 100 \text{ km}$. If, as is plausible, atomic oxygen is predominant in the region of the F_2 peak, one can proceed in a straightforward manner to construct a density profile of the neutral atmosphere at high altitudes from knowledge of the electron profile there.

Evidently for the better part of the day the presumed F layer is in a state of quasi-equilibrium; i.e., the change of electron (or ion) density per unit time is negligible compared to the change per unit time brought about by either production in photoionization or loss through recombination. This approximate balance is expressed as

$$(\sum_{\lambda} \sigma_{\lambda} I_{\lambda}) n(0) = \beta n(0+) \quad (21)$$

where $\sigma_{\lambda} \text{ cm}^2$ is the ionization cross section of oxygen at wave length λ , $I_{\lambda} \text{ photons cm}^{-2} \text{ sec}^{-1}$ is the solar flux at λ , and the summation extends over the spectral region effective in ionization ($\lambda < 910\text{\AA}$); $n(0)$ and $n(0+)$ are the respective number densities of neutral and ionized oxygen. The accepted value for $\sum_{\lambda} \sigma_{\lambda} I_{\lambda}$ is $\sim 10^{-7} \text{ sec}$. The loss coefficient β depends on the loss mechanism removing oxygen ions. In view of the likely composition of the Martian atmosphere the most plausible reaction appears to be the rearrangement



with a reaction coefficient $k' \approx 10^{-9} \text{ cm}^3/\text{sec}$. O_2^+ readily recombines in the dissociative recombination



In view of Equations (22) and (20)

$$\beta = k' n(\text{CO}_2) = D/H^2 \quad (24)$$

From kinetic theory it is found that

$$D = bT^{1/2}/n(0) \approx 10^{17} T^{1/2}/n(0) \quad (25)$$

assuming atomic oxygen to be the predominant constituent. The system of Equations (20) to (24) yields then for the atomic oxygen number density at the atmospheric peak

$$n(0) = \left[\frac{10^{17} n(0^+) T^{1/2}}{H^2 \Sigma \sigma_{\lambda} I_{\lambda}} \right]^{1/2} \quad (26)$$

Assuming oxygen to be the predominant ion in the region, $n(0^+)$ is equal to the observed electron density there. The neutral scale height, H , is half the observed plasma scale height, and knowledge of this parameter permits evaluation of the temperature, T , in this region. If, as Johnson⁽¹³⁾ and Fjeldbo et al⁽¹¹⁾ assume, the region above the peak is isothermal

$$T = \frac{m_o g}{k} H \quad (27)$$

With $m_o \approx 2.68 \times 10^{-23}$ gm, the mass of the oxygen atom, and $H \approx 12$ km, one obtains $T \approx 85^\circ$ K. Equation (26) yields then $n(0) \approx 10^9 \text{ cm}^{-3}$ at the ionospheric peak at 120 km.

The number density of CO_2 is then obtained from Equations (24) (25) and (26) and is given by

$$n(\text{CO}_2) = \frac{n(0) \Sigma \sigma_{\lambda} I_{\lambda}}{k' n(0^+)} \quad (28)$$

From the values of the various factors on the right side of Equation (28) the density of CO_2 at 120 km turns out to be $\sim 10^6 \text{ cm}^{-3}$. Down to an altitude where the ion density $n(0^+)$ vanishes, the above equations provide a density profile of CO_2 and 0, under the assumption that CO_2 is in diffusive equilibrium, i.e.,

$$n_z(\text{CO}_2) = n_{120}(\text{CO}_2) \exp \left[\int_z^{120} \frac{dz}{H(z)} \right] \quad (29)$$

which requires knowledge of the temperature profile for the evaluation of $H(z)$, the carbon dioxide scale height. Assuming the value of $\sim 10^6 \text{ cm}^{-3}$ for this component's density at 120 km

obtained above to be correct, the decrease of density by ~ 11 orders of magnitude from the surface density of $\sim 2 \times 10^{17} \text{ cm}^{-3}$ limits the average temperature between the two levels to low values.

Approximately,

$$10^{11} \approx \exp(120/\bar{H}) \approx \exp(2.43 \times 10^3/\bar{T})$$

or

(30)

$$\bar{T} \approx 95^\circ \text{ K}$$

where the bars denote averaged quantities.

The vapor pressure curve for CO_2 , on the other hand, provides a lower limit at all altitudes; otherwise an appreciable fraction of the CO_2 would condense and form dry ice. In this manner the observed atmospheric profile below 30 km is connected with the calculated profile above ~ 70 km. The results of such a calculation by Fjeldbo et al.⁽¹¹⁾ are presented in Figures 5 and 6. Johnson's results⁽¹³⁾ are very similar.

The salient features of this atmosphere are: 1) the very low temperature throughout the atmosphere, and 2) the low number densities, which lie at all altitudes well below the densities in the earth's atmosphere, e.g., $n(120) \approx 10^9$, compared to $\sim 5 \times 10^{11}$ at this altitude above the earth.

Though attractive in its simplicity, this model is subject to serious objections, leading to a radically different interpretation of the Mariner IV data⁽⁵⁾: 1) the conditions on T appear too stringent, and its value too low, in contrast to the results of radiative transfer calculations⁽¹⁰⁾. These show the middle atmosphere (up to ~ 60 km) to be in radiative equilibrium at temperatures substantially above the dry ice values, 2) isothermy in the ionosphere cannot be maintained by the radiative losses of CO_2 ; temperature gradients will build up, and a thermosphere with positive temperature gradients will be formed, and 3) the photochemical balance of the upper atmosphere is not considered in sufficient depth.

The latter argument led Chamberlain and McElroy to the conclusion that the atmosphere is not in diffusive equilibrium above ~ 70 km, but in a state of mixing up to high altitudes. Under these assumptions a very different atmospheric model can be constructed, as shown in the dashed curves in Figures 5 and 6. This model is characterized by substantially higher temperatures in the upper atmosphere, and by number densities which above 70 km exceed the terrestrial values. At 120 km, $n \sim 6 \times 10^{12} \text{ cm}^{-3}$ versus $\sim 5 \times 10^{11}$ on earth.

It should be noted that this model does not use directly the information, though limited, of the ionospheric density profile in deducing results about the upper atmosphere. Its proponents rather attempt to fit the empirical data on the ionosphere into the framework of their theoretical model, while using the empirical data near the surface as boundary values.

Consideration of the temperature and density at ~ 120 km leads the proponents of this model to the conclusion that the observed ionospheric layer is an E layer, analogous to the terrestrial E layer formed under similar ambient conditions. This permits calculation of the number density at the peak from Equation (19) assuming an approximate value for σ . Since σ varies with wavelength, this requires identification of the spectral range in the solar flux giving rise to photoionization. This is assumed to be soft X-radiation, leading to $\sigma \approx 10^{-19} \text{ cm}^2$, and $n \approx 5 \times 10^{12}$.

But this model also has to contend with a number of serious difficulties: 1) to provide mixing up to high altitudes one has to invoke a physical mechanism, such as eddy diffusion. But associated with the latter, eddy heat transport must be present, which would seriously affect the heat balance arrived at earlier without taking account of this mode of heat transport, and 2) the absence of an F layer higher up has to be explained in the presence of the ionizing agent - the UV radiation. To do so, unlikely high rate coefficients for the removal of ions in the high atmosphere are called for, e.g., a rate coefficient $k \approx 10^{-6} \text{ cm}^3/\text{sec}$ for the recombination of CO_2^+ .

Moreover the shape of the profile of the observed peak appears to fit well the theory of an F_2 layer. It is also the present writer's opinion that the strong diurnal variation inferred from Mariner IV results, but absent in the terrestrial F_2 region, may well be explained by the observed close proximity of the two ionization peaks on Mars, whose distance is only ~ 25 km, while on earth they are separated by ~ 200 km.

Since it appears that diffusion between the two regions is the factor governing the diurnal variation of the density profile⁽³⁰⁾, the short distance of separation between the two peaks may facilitate the rapid decay of electron and ion density after sunset.

An alternate interpretation of the observed ionospheric layer has been offered by Donahue⁽³¹⁾, who identifies the former as an F_1 layer, deducing an ambient density of $9 \times 10^{10} \text{ cm}^{-3}$ at $\sim 120 \text{ km}$, on the assumption of photoionization by EUV. The reduction in density from ground to this altitude leads then to an average scale height $\langle H \rangle \sim 8 \text{ km}$, whence the average temperature of a CO_2 atmosphere would be $\sim 150^\circ\text{K}$, a value more consistent with the results of radiative transfer calculations.

IV. SUMMARY AND SOME SUGGESTIONS FOR FURTHER STUDY

The survey of information on the Martian atmosphere in the preceding sections reveals the great uncertainty which still persists with respect to the atmospheric structure at high altitudes, whereas the order of magnitude of the relevant parameters near the ground appears now to be well established.

The greatest discrepancy between the various models exists in the estimate of densities and temperature in the upper atmosphere. The question arises how this deficiency in knowledge can best be removed, short of direct probing of these layers.

It appears that the first task to be performed is a renewed effort at constructing a more unified theoretical model of the Martian atmosphere, incorporating the knowledge gained from the Mariner IV flyby, and including a consistent treatment of the ionosphere. The latter may serve as a test in discriminating between the various possibilities. Existing models inevitably were a patchwork of calculations using input parameters of questionable validity, dependent on unknown boundary values of temperature and pressure, and on an unknown composition. These parameters can now be much better defined. If possible, attempts should be made to obtain a rough idea of diurnal and seasonal and other variations of the ionosphere.

This appears to be essential in preparation for proper evaluation of prospective data to be expected from additional flybys and possible Martian orbiter missions which have been suggested as a further step in exploring the Martian atmosphere.

In addition to occultation measurements the possibility of topside sounding of the ionosphere should be studied. The temporal and spatial dependence of ionospheric structure may offer a clue to the actual character of the observed charged layer, and therefore, enable a better definition of neutral atmospheric structure:

- 1) Evidently correct identification of the type of ionospheric layer determines quite unambiguously the order of magnitude of the ambient atmospheric density, as can be inferred from the great difference in density of the simple tentative models described in Section 3.
- 2) On earth the different types of layer exhibit different diurnal variation, as mentioned in Section 3. Though the details of the variation on Mars may differ from those on earth, it can be expected that the difference in behavior between the distinct types will not be wiped out on Mars.
- 3) The same holds for the spatial variation of the different layers. On earth, in view of diffusion in the magnetic field, the F_2 layer shows variations strongly correlated with geomagnetic position. Though an upper limit has been established for the Martian magnetic field $\leq 10^{-3}$ that of the earth, even a weak field may have effects on the structure of an F layer. This field, if present, may be amenable to detection by an orbiting satellite with a periapsis of ~ 1000 km. Thus, observed spatial variations in the ionosphere and correlation with the magnetic field of Mars may help in identification.
- 4) A similar statement can be made about variation with solar cycle. On earth the strongest relative variability with solar cycle is displayed by the nighttime F_2 layer compared to the nighttime E layer, where little or no changes can be seen between solar maximum and minimum (see e.g., Figure 4.2 in⁽³⁰⁾).

Another possible step in the study of the Martian atmosphere may be further spectroscopic study from a satellite-based observatory free of the disturbing effects of the terrestrial atmosphere. Such a study may narrow the uncertainty in abundance of minor components such as CO , O_2 , and O , whose relative abundance may offer insight into the character of the transition from mixing to diffusive separation.

Obviously a final answer to the problem of the Martian upper atmosphere will have to wait until direct probing of the atmosphere can be effected in close (~ 200 km) flyby. But considerable progress is possible earlier if a concerted effort of study is made in the right direction.

A number of special problems touching on the structure of the Martian atmosphere exist which have not been treated in this review such as, for instance, the problem of Blue Haze, the question of life, etc. It is felt, however, that a better definition of the general atmospheric structure has to precede the solution of these questions, since clearer insight into the former will eliminate a number of suggested solutions for the latter. In view of this, the preceding survey has been restricted to "purely" atmospheric problems.

The author wishes to thank Messrs. B. T. Howard, D. B. James, and W. B. Thompson who have aroused his interest in the subject.

M. Liwshitz (by W.B.T.)

1012-ML-csh

M. Liwshitz

Attachments:

References

Figures 1 - 6

Copy to

(see next page)

Copy to

NASA Headquarters

Messrs. P. E. Culbertson - MTL
J. H. Disher - MLD
F. P. Dixon - MTY
E. Z. Gray - MT
T. A. Keegan - MA-2
D. R. Lord - MTX
M. J. Raffensperger - MTE
L. Reiffel - MA-6
A. D. Schnyer - MTV
W. B. Taylor - MLA

Manned Spacecraft Center

M. A. Silveira - ET25
W. E. Stoney, Jr. - ET
J. M. West - AD

Marshall Space Flight Center

R. J. Harris - R-AS-VP
B. G. Noblitt - R-AERO-XA
F. L. Williams - R-AS-DIR

Kennedy Space Center

J. P. Claybourne - EDV4
R. C. Hock - PPR2
N. P. Salvail - MC

Bellcomm, Inc.

G. M. Anderson
C. L. Davis, Jr.
J. P. Downs
D. R. Hagner
P. L. Havenstein
J. J. Hibbert
W. C. Hittinger
B. T. Howard
D. B. James
H. S. London
R. K. McFarland
K. E. Martersteck
J. Z. Menard
I. D. Nehama
G. T. Orrok
I. M. Ross
R. L. Selden
R. V. Sperry
J. M. Tschirgi
R. L. Wagner
All members, Division 101
Department 1023
Library
Central File

BELLCOMM, INC.

REFERENCES

1. Sinton, N. M. and J. Strong, Ap. J. 131, 459, 1960.
2. de Vancoeurs, G., in Proc. of the 3rd. Intern. Symp. on Bioastronautics and Exploration of Space, U.S.A.F., 1956.
3. Kliore, A. et al., Science, 149, 1243, 1965.
4. Kaplan, L. D. et al., Ap. J. 139, 1, 1964.
5. Chamberlain, J. W. & D. M. Hunten, Rev. Geophys. 3, 299, 1965.
6. Dollfus, A., Comp. Rend. Ac. Sci, Paris, 256, 3009, 1963.
7. Goody, R. M., Weather, 12, 3, 1957.
8. Chamberlain, J. W., Ap. J. 136, 582, 1962.
9. McElroy M. B., et al., Ap. J. 141, 1523, 1965.
10. Prabakhara, C. and J. S. Hogan, J. Atmos. Sci. 22, 97, 1965.
11. Fjeldbo, G. et al., J. Geophys. Res., 71, 2307, 1966.
12. Chamberlain, J. W. and M. B. McElroy, Science, 152, 21, 1966.
13. Johnson, F. S., Science, 150, 1445, 1965.
14. Johnson, F. S., preprint of a paper presented at the 7th COSPAR Symp. in Vienna, Austria, May 1966.
15. Gross, S. H., et al., Science, 151, 1216, 1966.
16. Sinton, W. M., in the Solar System III, Satellites and Planets, ed. by G. P. Kuiper and B. M. Middlehurst, p. 429, the University of Chicago press, Chicago and London, 1961.
17. Opik, E. J. in Progress in the Astronautical Sciences, ed. by S. F. Singer, p. 263, North Holland, Amsterdam, 1962.
18. Mintz, in Studies of the Physical Properties of the Moon and Planets, p. 81, Tech. Rep. RM-2769-JPL, Rand Corp., 1961.
19. Giorduaire, J. A., Proc. IRE, 47, 1062.
20. Mayer, C. H., in The Solar System III Satellites and Planets, ed. by G. P. Kuiper and B. M. Middlehurst, p. 442, the Univ. of Chicago Press, Chicago and London, 1961.

21. Gold, E., Proc. Roy. Soc. A 82, 43, 1909.
22. Humphreys, W. J., Ap. J. 29, 14, 1909.
23. Green, A.E.S. and R. J. Wyatt, Atomic and Space Physics, Addison-Wesley, Reading, Mass., 1965.
24. Goody, R. M., Atmospheric Radiation, I. Theoretical Basis, Oxford, Oxford, 1964.
25. Spencer, D. F., in AIAA/AAS Stepping Stones to Mars Meeting, p. 532, AIAA, New York, 1966.
26. Kliore, A. and D. A. Tito, in AIAA/AAS Stepping Stones to Mars Meeting, p. 5, AIAA, New York, 1966.
27. Fjeldbo, G. and V. R. Eshleman, J. Geophys. Res. 70, 3217, 1965.
28. Fjeldbo, G. et al., J. Geophys. Res., 70, 3701, 1965.
29. Johnson, F. S., in Progress in the Astronautical Sciences, ed. by S. F. Singer, p. 51, North-Holland, Amsterdam, 1962.
30. Hanson, W. B. and T. N. L. Patterson, Planet, Space Sci., 12, 979, 1964.
31. Donahue, T. M., quoted in (14).

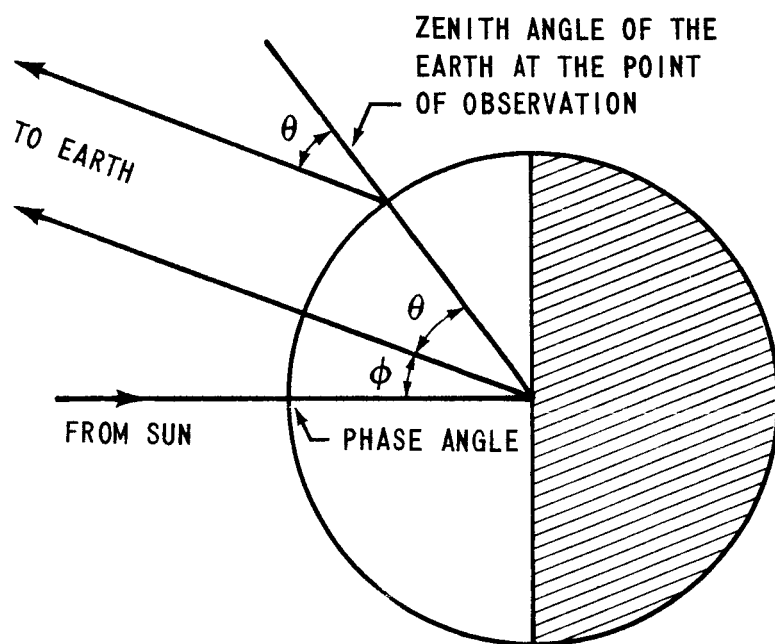
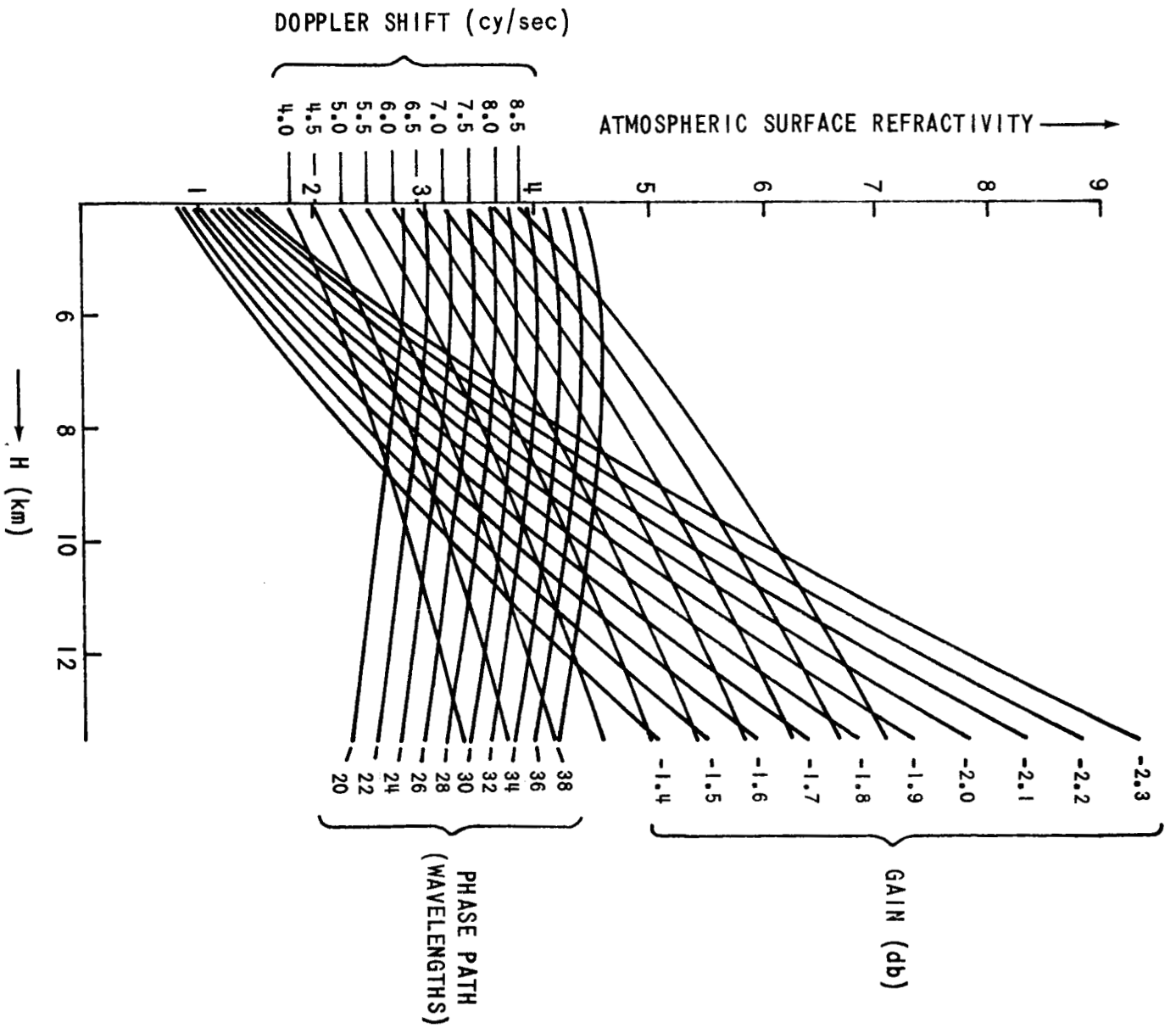


FIGURE 1 - RELEVANT ANGLES IN ASTRONOMICAL OBSERVATIONS OF PLANETS

FIGURE 2 - MAXIMUM CHANGES OF PHASE, GAIN, AND FREQUENCY IN RELATION TO REFRACTIVITY AND SCALE HEIGHT OF MODEL ATMOSPHERES



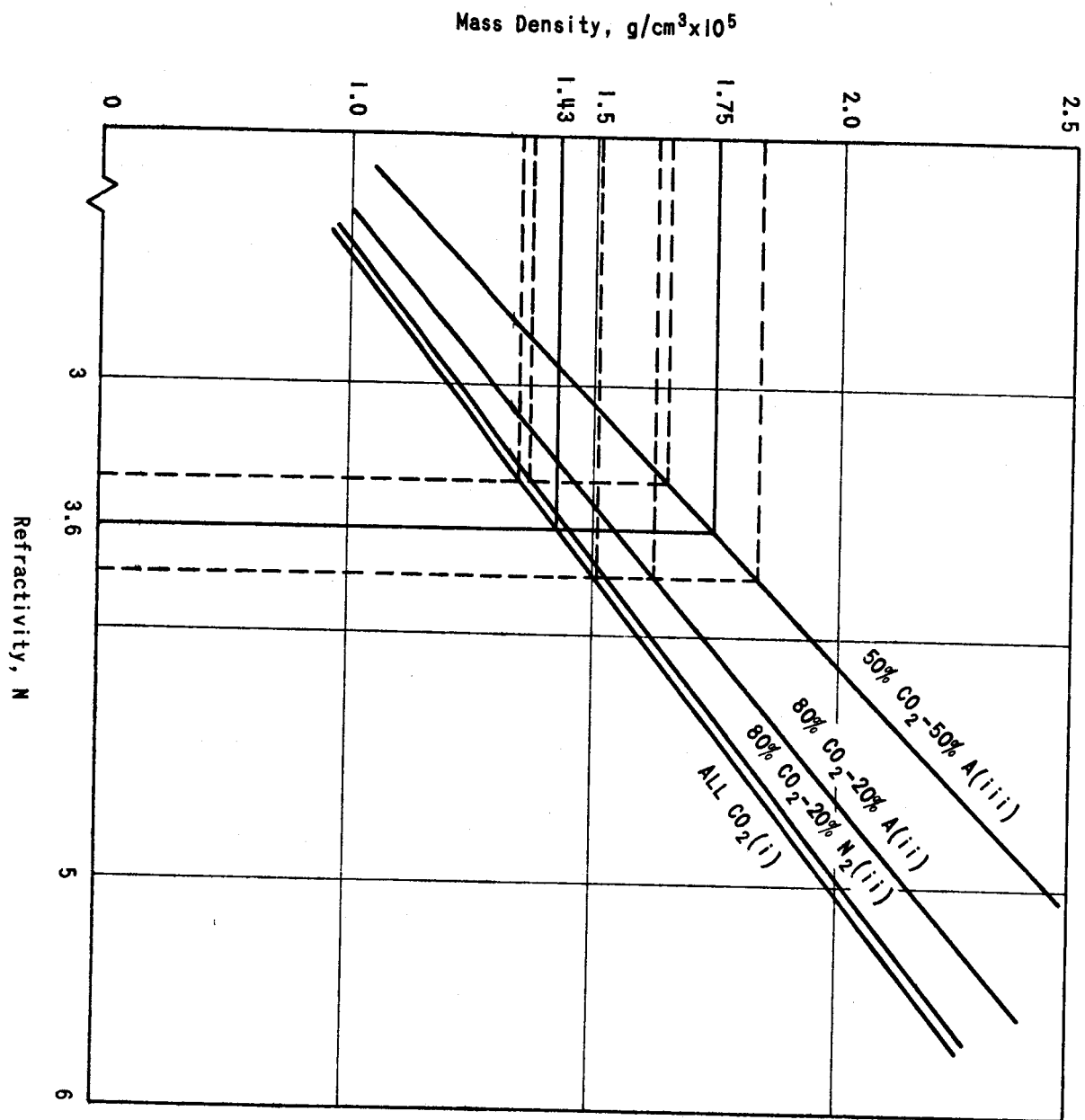


FIGURE 3 - REFRACTIVITY AND MASS DENSITY AS A FUNCTION OF ATMOSPHERIC COMPOSITION

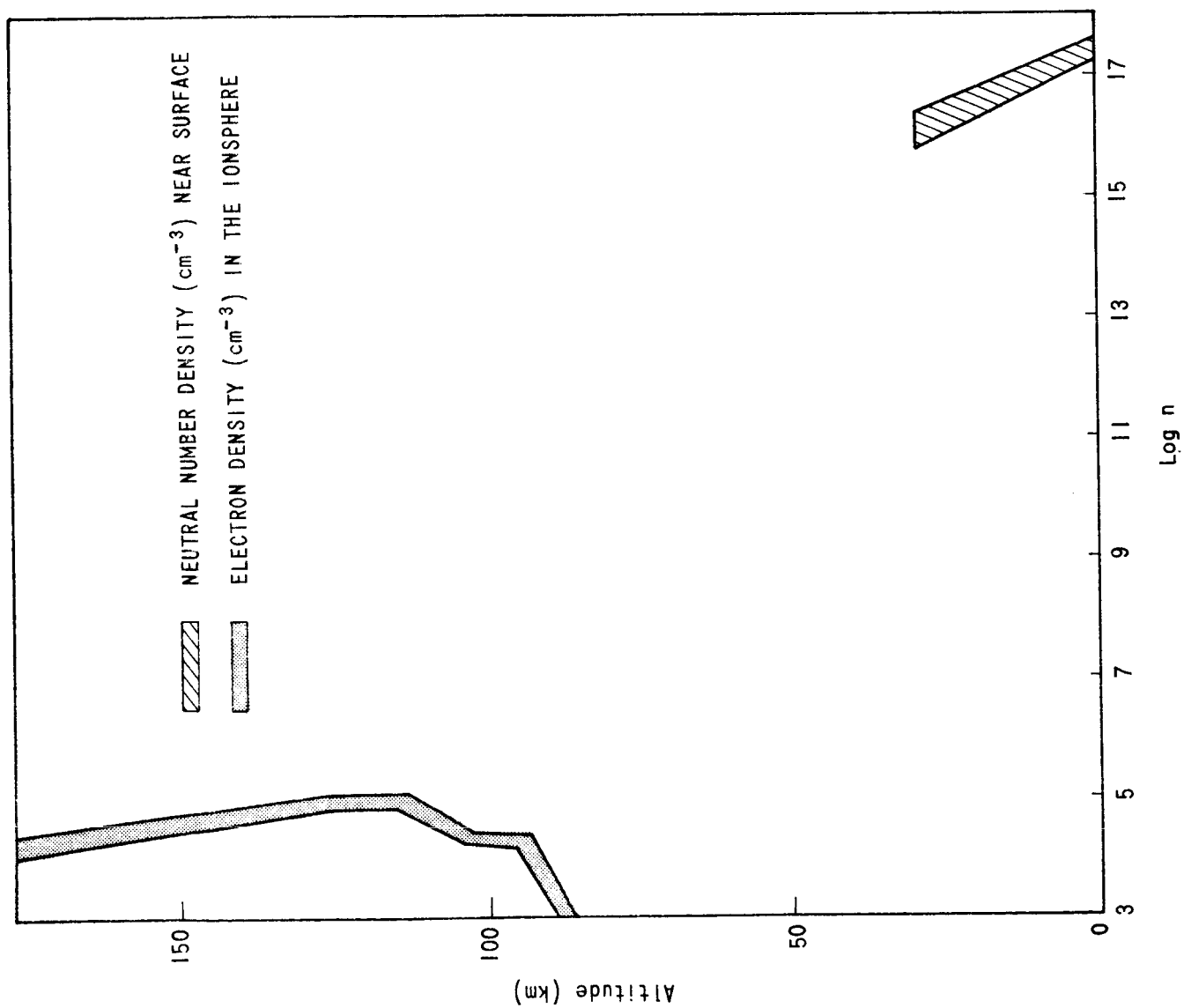


FIGURE 4 - RESULTS OF MARINER IV

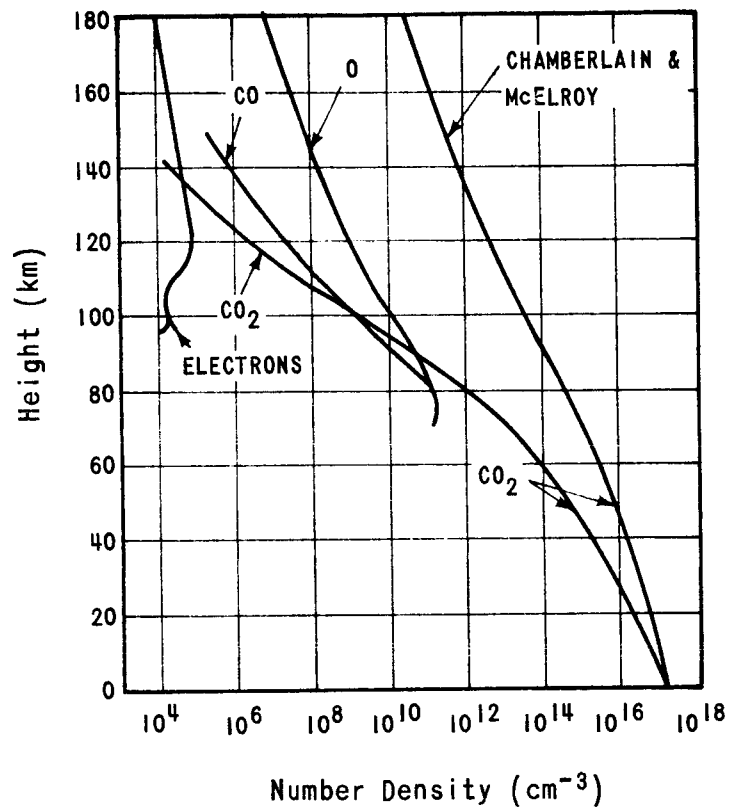


FIGURE 5 - MODELS OF MARTIAN ATMOSPHERIC
NUMBER DENSITY. EXTREME RIGHT
CURVE - CHAMBERLAIN AND McELROY.
ALL OTHER CURVES - FJELDBO ET AL.

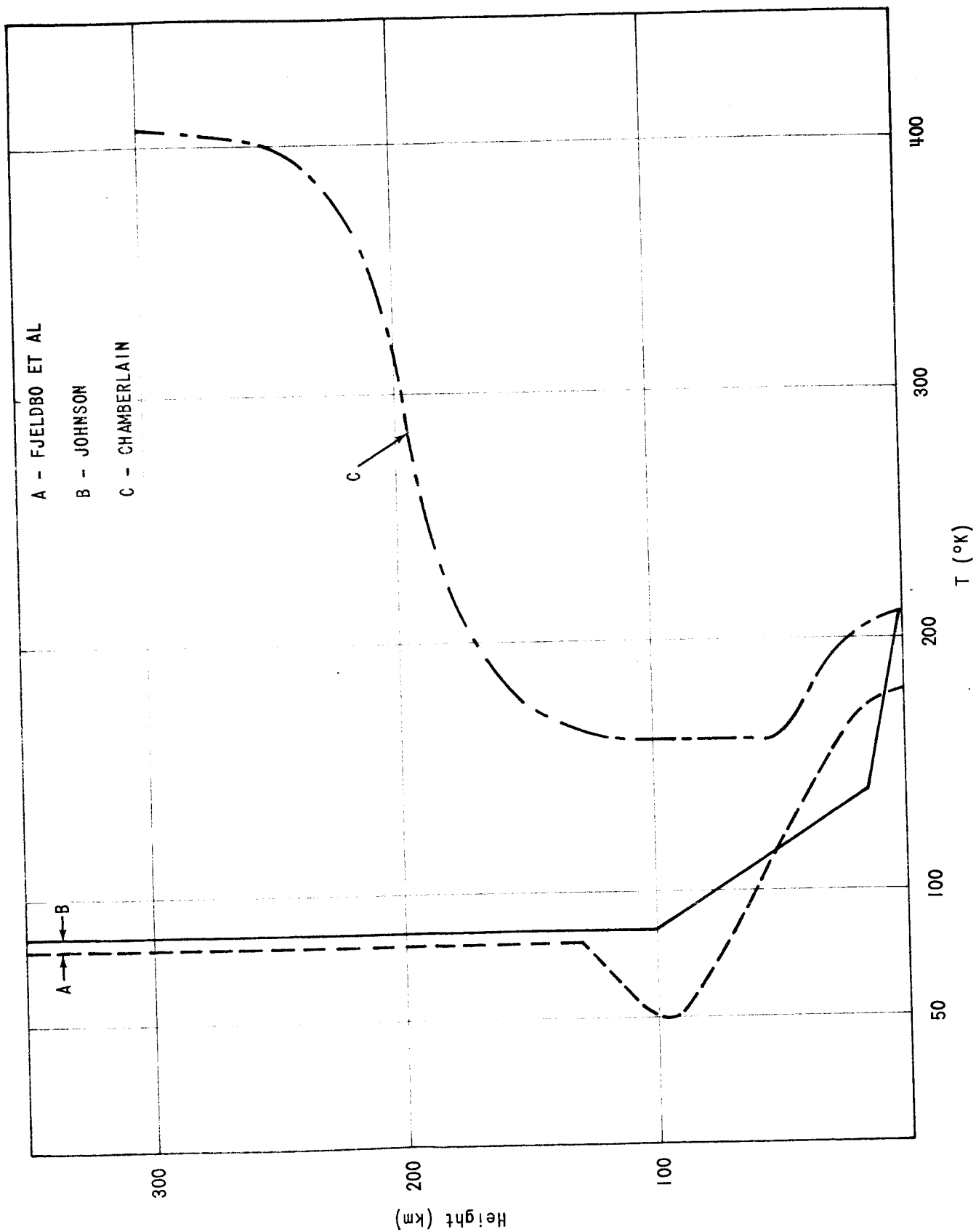


FIGURE 6 - MODELS OF MARTIAN TEMPERATURE PROFILE

00825

3 up

25-1-67